



# The role of vaccination roll-out in the monitoring of Covid-19 pandemic spread: A country-level quantitative study<sup>☆</sup>

Arianna Agosto <sup>a</sup>, Paola Cerchiello <sup>a</sup>, Siegfried Eisenberg <sup>b</sup>,  
Thomas Czipionka <sup>b,c</sup>

<sup>a</sup> University of Pavia, Dep. of Economics and Management, Pavia, 27100, Italy

<sup>b</sup> Institute for Advanced Studies, Research Group Health Economics and Health Policy, Vienna, 1080, Austria

<sup>c</sup> London School of Economics, London, UK

## ARTICLE INFO

Dataset link: <https://github.com/owid/covid-19-data/tree/master/public/data>

### Keywords:

Covid-19 pandemic  
Reproduction rate  
Vaccination roll-out  
Explosivity tests  
Pandemic monitoring

## ABSTRACT

Early detection of contagion surge phases that could potentially mark the beginning of new waves is crucial to monitor the pandemic development and to define proper health policies. The potential availability of reliable covariates can effectively support the monitoring of the pandemic development and provide early warning signals.

This paper combines epidemic surge detection with the study of the role of vaccination roll-out, by improving and enhancing the methodology introduced by Agosto and Cerchiello (2024). A covariate-augmented version of the BSADF test for the detection of explosive patterns in time series, named CBSADF test, is used to identify whether the time series of the effective reproduction number moves to explosive behavior, indicating a potential upcoming wave, conditioned on the evolution of the vaccination roll-out.

By applying our method to a representative set of European countries, we show that the model can effectively identify upcoming exponential increases in the effective reproduction number and the interplay with the vaccination roll-out.

## 1. Introduction

Reliable information about the severity of an illness, its transmissibility, its speed of transmission, and population groups at risk are some of the main needed parameters to evaluate the upcoming burden of epidemic spread and to choose appropriate measures to control it [1]. Measures can be divided into pharmaceutical - vaccinations and pharmacotherapy - and non-pharmaceutical ones - social distancing, school closures, business restrictions - and they are chosen according to the overall strategy of containment or mitigation. Introducing appropriate measures at an early stage of a pandemic has been shown to result in a lower number of necessary and most likely less restrictive measures compared to taking measures at a later stage [2,3].

In the present paper, we propose a statistically sound and data-driven protocol to detect critical phases in the pandemic patterns – potentially corresponding to new contagion waves – by leveraging the dynamic relationship between reproduction rate and vaccination roll-out. Our approach is based on an econometric test applied to the reproduction rate and vaccination roll-out time series. By using the number of new vaccinations as covariate in our testing procedure, we are able to provide an early warning signal of critical surge phases during pandemics and to assess whether and when the vaccination roll-out plays a more decisive role in determining such signal.

<sup>☆</sup> This article is part of a Special issue entitled: 'Inequalities' published in Physica A.

\* Corresponding author.

E-mail addresses: [arianna.agosto@unipv.it](mailto:arianna.agosto@unipv.it) (A. Agosto), [paola.cerchiello@unipv.it](mailto:paola.cerchiello@unipv.it) (P. Cerchiello).

<https://doi.org/10.1016/j.physa.2025.131160>

Available online 3 December 2025

0378-4371/© 2025 The Authors. Published by Elsevier B.V. This is an open access article under the CC BY-NC-ND license (<http://creativecommons.org/licenses/by-nc-nd/4.0/>).

**Table 1**

For each country and contagion rise phase, we provide the variable indicating whether the test with covariate signals the explosive pattern, codified as follows: ‘0’ no signal ( $p$ -value higher than 10%); ‘1’ signal ( $p$ -value lower than 10%); ‘quasi-signal’ ( $p$ -value higher than 10% but considerably dropping). In parentheses, we report the number of days the explosiveness signal stayed active.

Country	Delta wave	Omicron wave	Summer 2022 rise
Austria	quasi-signal	0	1 (9)
Bulgaria	1 (27)	1 (12)	1 (16)
Czechia	1 (7)	1 (12)	1 (5)
Denmark	1 (18)	1 (6)	1 (41)
France	quasi-signal	1 (42)	1 (15)
Germany	1 (14)	0	1 (7)
Italy	1 (9)	1 (8)	quasi-signal
Poland	1 (26)	1 (8)	1 (21)
Portugal	1 (25)	1 (8)	1 (32)
Spain	1 (8)	1 (26)	1 (6)
Sweden	quasi-signal	1 (7)	1 (26)
United Kingdom	1 (49)	1 (11)	1 (12)

Our approach can become an additional tool to assist policy-makers and epidemiologists in shaping and adapting decisions regarding containment measures.

The protocol foresees:

- the specification of the test itself, by identifying the variables to be used, more specifically the ideal covariate;
- the methodology to isolate and date stamp the beginning of an explosive phase thanks to the employed covariate;
- the effective comparison between the test with and without covariate as to underline the comparative advantages;
- a set of results that offers more ready-to-be-used and insightful indications that could not be identified with other strategies, (like Granger causality test);
- the avoidance of endogeneity issues as they are naturally addressed by the approach itself.

Considering the above-mentioned modeling protocol, we focus our interest on the process of the daily number of new vaccinations, which can be considered as a proxy of the speed of vaccination roll-out. The decision to use vaccination as covariate in the current modeling framework derives from the ascertainment that it represents the only tool able to eradicate a virus disease. NPIs are instead used to contain the spread and the acceleration of a pandemic when either vaccination roll-out or effective pharmaceutical treatments are not available. We also acknowledge that the recent field literature has extensively analyzed the role of NPIs, thus we would rather elicit the specific role played by the vaccination roll-out. Moreover, it should be noticed that the relationship between effective reproduction number and vaccinations is expected to be two-way. On the one hand, vaccination roll-out should contain the contagion growth, with a variable effect depending on the different virus variants. On the other hand, during pandemic waves, there is an increasing incentive for the national authorities to accelerate the vaccination roll-out, and, for private individuals, to get immunization. However, this does not constitute an issue for the modeling framework proposed in the present work, rather a careful inspection and interpretation of the results is needed.

The CBSADF test is applied to the time series of effective reproduction numbers in ten different European countries, to investigate whether the test reveals explosive phases and validate whether this information provides a temporal advantage compared to considering only the development of the newly confirmed cases. Ideally, the test should provide a warning signal at an early stage of the new cases surge phase and before its peak. Indeed, the CBSADF test for time series analyses of epidemiological parameters represents a promising methodology to alert policymakers at an early stage of a critical development of the spread of infectious diseases and, consequently, reveals if increases in contagion speed are meaningful or most likely due to random fluctuations.

Additionally, the proposed approach can be applied with low effort and fewer assumptions in the analysis of the evolution of other epidemiological parameters or human behaviors like the number of deaths and the number of recovered.

Our results indicate that the proposed testing approach represents an effective tool to monitor the pandemic pattern, as it provides a reliable signal for the identification of potential new waves.

In this respect and to summarize our findings, Table 1 reports the signal provided by our test in three periods characterized by a strong growth of new infections: spring/summer 2021, occurring with the spread of Delta variant, end of 2021/beginning of 2022, corresponding to the so-called Omicron wave, and summer 2022, when a rise of cases was observed in most countries. It can be noticed that, as discussed in detail in Section 4, in nearly all cases the test provides a signal (indicated as ‘1’ in the table, with the number of active signal days shown in brackets) or a ‘quasi-signal’ of the on-going acceleration of the reproduction rate. The definition and calculation of signals is detailed in Section 2 and refers to the  $p$ -value of the test (a  $p$ -value below or rapidly approaching a certain threshold produces a signal and a quasi-signal respectively).

Since our testing framework includes the progress of national vaccination as a covariate, these findings suggest that vaccination roll-out can represent an alert warning tool for contagion surge phases.

In Section 2, the theoretical approach to identifying possible explosive behaviors in the time series of epidemiological parameters is explained. In Sections 3 and 4, we present the data and empirical results for ten European countries, respectively, and thereafter discuss the ability of the explosivity test in the context of retrospective epidemiological data and measures and patterns of signals across countries. Section 6 concludes.

## 2. Methodology

To early predict the spread and burden of diseases, different kinds of mathematical models, following different approaches, have been established in the last decades [4]. One of the first approaches has been SIR models that are based on the division of the population into groups according to different health status stages denoted as ‘Susceptible’ (S), ‘Infectious’ (I) and ‘Recovered’ (R). Depending on different rates and probabilities, the population is expected to process through those three stages [5]. Another common approach in epidemiology is agent-based computer simulations that model the behavior of individuals (‘agents’) considering different attributes, e.g., exposure to a disease, to estimate outcomes like number of infections or deaths among all agents who represent a specific population group [6,7]. During the SARS-Cov-2 pandemic, these two types of models were often used to simulate and predict the impact of (non-)pharmaceutical interventions on the spread of the disease and derive policy recommendations [8,9]. Additionally, the increasing availability of large datasets about human behavior has led to innovative approaches like using mobility data provided from smartphone GPS data, analyzing data streams, e.g., Twitter/X activities or Google Searches, to predict the spread of the disease [10,11] or wastewater analyses to reveal the circulating amount of virus copies [12]. Furthermore, in an attempt to enable country comparisons of epidemic waves in retrospect, Harvey et al. [13] proposed an algorithm that measures maxima and minima values along the epidemic curve.

However, while the scope of mathematical models is to predict the future development of a pandemic for different scenarios, based on estimated epidemiological parameters and additional assumptions, the idea of retrospective analyses is to evaluate which measures are most effective in different epidemic phases and to give recommendations for future outbreaks. Consequently, prognoses aim for future predictions or retrospective evaluations, while a feasible method to evaluate whether there is a current need for action is still lacking. Recently, Agosto and Cerchiello [14] proposed an approach that is able to detect potentially critical phases by modeling the time series of the effective reproduction number via a proper econometric technique. In their paper, the authors apply a time series test known as Backward Supremum Augmented Dickey Fuller (BSADF) test, which allows revealing whether the development of the effective reproduction number has switched to “explosive” behavior, a regime of extremely rapid growth, mathematically represented [15] by a submartingale process that is expected to only increase in time. The start of such a phase gives a signal that requires further consideration of the epidemic situation. Indeed, the authors acknowledge one specific limitation in their approach: no further source of variability or extra information, apart from the effective reproduction number, is taken into account. That is the reason why, in the present study, we consider an improved version of the BSADF test, the covariate-augmented version of the BSADF test, named CBSADF [16], based on repeated estimation of the covariate-augmented ADF (CADF) test statistic by Hansen [17]. Astill et al. [16] showed that including covariates whose dynamic is significantly correlated with the tested time series improves the performance of explosivity tests, thanks to a more accurate estimate of the autoregressive coefficient. In particular, such improvement occurs when there is a significant (and possibly mutual) relationship between the covariate and the target time series, in terms of contemporaneous correlation and/or Granger causality.

Unit root tests are widely used in the statistic and econometric literature to verify the hypothesis that a time series evolves according to a random walk against the alternative hypothesis that it follows a stationary autoregressive process. In unit root processes, the effect of a shock that occurred at a given time persists indefinitely in the future, with several consequences in terms of statistical properties and parameter estimation. In fact, the autocovariance structure of a unit root process changes in time, while in stationary processes it does not.

Unit root tests based on Augmented Dickey Fuller (ADF) regression [18] are very common in financial applications, as financial price time series typically follow random walk processes. In the financial context, it is also relevant to conduct unit root tests against the alternative hypothesis that a series follows an explosive process, characterized by exponential growth. These so-called right-sided unit root tests (or *explosivity* tests) are typically applied to detect speculative bubbles in financial markets [19–21].

We propose using the same approach to monitor changes in the COVID-19 contagion dynamics. Indeed, while stationarity phases in the effective reproduction number time series should correspond to periods of stability in the number of new infections, and unit root phases (so-called random walks) should indicate periods of contagion growth, the extremely rapid increase in the effective reproduction number characterizing the spread of new COVID-19 waves can be described by the exponential growth (*explosivity*), whose detection is the objective of the tests considered in the paper.

Moving to the technical definition of our testing procedure, let us first recall the ADF statistics, based on the following regression:

$$\Delta y_t = \mu + \phi y_{t-1} + \sum_{i=1}^p \psi_i \Delta y_{t-i} + \varepsilon_t, \quad \varepsilon_t \sim i.i.d.(0, \sigma^2) \quad (1)$$

where  $\mu$  is the intercept and  $p$  is the number of lags of the differenced dependent variable  $\Delta y_t$ , with associated coefficients  $\psi_i$ . Alternative specifications of the ADF test can be obtained by imposing the constraint  $\mu = 0$  (no-constant case) and/or including a trend component.

In the standard ADF test, Eq. (1) is used to test the null hypothesis  $\phi = 0$ , corresponding to the random walk process, against the alternative of stationarity ( $\phi < 0$ ).

In the right-tailed unit root test for explosivity proposed by [22], the null hypothesis is still the random walk one, but the alternative is  $\phi > 0$ , corresponding to explosive behavior. In particular, Phillips et al. [22] proposed a backward-superior ADF test, named BSADF, based on repeated estimation of the ADF test statistic using a forward and backward rolling-windows technique, to allow for date-stamping of explosive phases (so-called “bubbles” in the financial context). Specifically, defining  $r_0$ ,  $r_1$  and  $r_2$   $\in [0, 1]$  as fractions of the total sample length  $T$ , the endpoint of each sample is fixed at  $r_2$  (the sample fraction corresponding to

the endpoint of the window), while the start point varies from 0 to  $r_2 - r_0$  (the sample fraction corresponding to the origination of the window):

$$BSADF_{r_2} := \sup_{r_1 \in [0, r_2 - r_0]} \{ADF(p)_{r_1}^{r_2}\} \quad (2)$$

According to Eq. (2), at every  $r_2 T$  time (day), the BSADF value is defined as the maximum ADF value calculated over intervals expanding from  $[0, r_2]T$  to  $[r_2 - r_0, r_2]T$ , where  $r_0 T$  is the minimum window width chosen by the analyst to ensure that all the considered sub-series have a sufficient length to make the test results consistent. Thus, at each window end time  $r_2 T$ , the BSADF test statistic is the supremum of the right-tailed ADF statistics computed on all subsamples ending at date  $t$  subject to a minimum sample size  $[r_0 T]$ . Based on this approach, defining  $r_{s,ADF} \in [0, 1]$  and  $r_{e,ADF} \in [0, 1]$ , the estimated origination date of an explosive phase  $\hat{r}_{s,ADF}$ , expressed as a fraction of the total sample length  $T$ , is calculated as the first time in which the calculated BSADF statistic exceeds the critical value, while the first following observation whose BSADF statistic goes back below the critical value is considered as the termination date ( $\hat{r}_{e,BSADF}$ ) of the same bubble:

$$\hat{r}_{s,BSADF} = \inf_{r_2 \in [0, 1 - r_0]} \left\{ r_2 : BSADF_{r_2}(r_0) > cv_{r_2}^\alpha \right\} \quad (3)$$

$$\hat{r}_{e,BSADF} = \inf_{r_2 \in [r_s, 1]} \left\{ r_2 : BSADF_{r_2}(r_0) < cv_{r_2}^\alpha \right\} \quad (4)$$

where  $cv_{r_2}^\alpha$  is the critical value of the BSADF statistic at time  $r_2$  for the significance level  $\alpha$ .

Critical values for the BSADF test can be obtained through simulation experiments based on the limiting distribution in [22] or through the bootstrap approach proposed by [16].

Astill et al. [16] extended this approach to account for the role of covariates, by proposing a covariate-augmented version of the BSADF test, named CBSADF, based on repeated estimation of the covariate-augmented ADF (CADF) test statistic by [17].

Hansen [17] assumes that the time series to be tested for a unit root can be written as:

$$\Delta y_t = \tilde{\mu} + \tilde{\phi} y_{t-1} + \sum_{i=1}^p \tilde{\psi}_i \Delta y_{t-i} + \sum_{i=1}^q \xi_i \Delta x_{t-i} + \tilde{\epsilon}_t, \quad \epsilon_t \sim i.i.d.(0, \sigma^2) \quad (5)$$

where  $x_t$  is a stationary covariate process.

In the CADF test based on Eq. (5), the null hypothesis is, as in the ADF test, that  $\tilde{\phi} = 0$ , corresponding to the random walk case, against the alternative of stationarity ( $\tilde{\phi} < 0$ ). As in the no-covariate case, alternative specifications can be obtained by setting the constant parameter equal to 0 and/or including a trend component. Hansen [17] showed that the CADF test is expected to have more power than the ADF one when the  $x_t$  and the  $y_t$  processes are significantly related, because, in this case, the error variance is lower than in the univariate regression (1). The inclusion of covariates may affect not only the standard error but also the estimate of the  $\phi$  autoregressive coefficient. The extent of the power gain depends on the contemporaneous and temporal correlation structure between the tested time series  $y_t$  and the  $x_t$  covariate, as shown in [23].

Astill et al. [16] proposed and studied the right-tailed version of the CADF test, based on the application of the same forward and backward rolling-windows technique described for the BSADF test. Specifically, at each window end time  $r_2$ , the CBSADF test statistic is the supremum of the right-tailed CADF statistics computed on all subsamples ending at date  $t$  subject to a minimum sample size  $[r_0 T]$ :

$$CBSADF_{r_2} := \sup_{r_1 \in [0, r_2 - r_0]} \{CADF(p)_{r_1}^{r_2}\} \quad (6)$$

Analogously to the BSADF testing procedure, the origination date of an explosive phase ( $\hat{r}_{s,CADF}$ ) is calculated as the first time in which the CBSADF statistic exceeds the critical value, while the first observation following ( $\hat{r}_{e,CBSADF}$ ) whose CBSADF statistic goes back below the critical value is considered the termination date ( $\hat{r}_{e,CBSADF}$ ) of the same bubble:

$$\hat{r}_{s,CBSADF} = \inf_{r_2 \in [0, 1 - r_0]} \left\{ r_2 : CBSADF_{r_2}(r_0) > cv_{r_2}^\alpha \right\} \quad (7)$$

$$\hat{r}_{e,CBSADF} = \inf_{r_2 \in [r_s + \delta T, 1]} \left\{ r_2 : CBSADF_{r_2}(r_0) < cv_{r_2}^\alpha \right\} \quad (8)$$

Astill et al. [16] show that the CBSADF test outperforms the BSADF one, from a statistical point of view, in terms of both power and size. The test statistics calculated with the two tests can be substantially different when the covariate and the error term of the target time series are significantly correlated. Indeed, the assumptions of the CBSADF test allow for a mutual relationship between the tested time series and the covariate process. In particular, the specification by Hansen [17] is equivalent to assume that the tested and the covariate time series form a Vector AutoRegressive (VAR) model. The strength of the relationship between the two series entering the VAR model determines the possible performance improvement obtained by including the covariate in the testing procedure. Specifically, Caporale and Pittis [23] showed that a more precise estimate of the autoregressive coefficient, on which the unit root tests are based, is attained when a significant contemporaneous correlation between the shock component of the two series is in place or when one of the two series Granger-causes the other. Indeed, the covariate is not assumed to be exogenous, as Granger-causality can occur in both directions (from the covariate to the tested series and/or vice-versa).

The above-presented CBSADF test has been employed in financial contexts, as explosive patterns typically occur with market prices. Our proposal is to exploit the CBSADF testing approach within a completely different context, that is, with the effective



reproduction number of COVID-19, providing both a signal that the policymaker can use to anticipate epidemic waves and an ex post tool to analyze the impact of vaccination in containing the spread of the disease.

Indeed, the backward-expanding rolling window technique allows a daily update of the monitoring tool, while, at the same time, taking into account the history of the national pandemic evolution. In our empirical study, we apply the described explosivity test to the effective reproduction number time series in each of the considered countries both without covariates (BSADF test) and using the daily number of new vaccinations as a covariate (CBSADF test). Our main aim is to identify the start of new waves in different countries: in both tests, the presence of a  $p$ -value lower than the chosen significance level means that the null hypothesis of a random walk for the effective reproduction number series is rejected in favor of the alternative hypothesis of explosivity. By comparing the results obtained with the two tests (with and without covariate), we also shed light on how the impact of vaccination roll-out on the contagion dynamics changes over time. Indeed, the two tests are expected to provide the same signal when the mutual relationship between effective reproduction number and vaccination is not significant, while they could diverge – and potentially lead to different conclusions – when such relationship is significant. In the second case, the CBSADF test provides a potentially different signal from BSADF one, and represents a more accurate monitoring tool of the pandemic evolution.

### 3. Data and preliminary analysis

We consider the dataset from the OurWorldInData (OWID) data repository, that comprises different and regularly updated epidemiological data from several sources, e.g., WHO, official data collected by the OWID team, and, additionally, estimated parameters like the effective reproduction number. In particular, in the present study we consider the following time series: the ‘reproduction rate’, also called the ‘effective reproduction number’, the ‘new vaccinations smoothed per million’, and the ‘Stringency Index’. While the notation ‘smoothed’ indicates that the number is a 7-day average and ‘per million’ refers to the fact that numbers are standardized by country population size, the effective reproduction number represents a real-time estimate based on the approach by Arroyo-Marioli et al. [24], and generally indicates an increase in newly confirmed cases if  $> 1$  and a decrease in newly confirmed cases if  $< 1$ . The effective reproduction number  $R_t$  is the expected number of cases produced by one infected person at time  $t$ . In a fully susceptible population, it is called  $R_0$ , the basic reproduction number.  $R_t$  increases or decreases due to biological (mutation, population immunity) or social reasons, e.g. implementation of NPIs.

In both the BSADF and the CBSADF test performed in our empirical study (Section 4), the dependent (tested) variable is the effective reproduction number, while the covariate used in the CBSADF test is the 7-day lagged variation (first differences) of the smoothed daily number of administered vaccine doses. Using the differenced variable allows us to rely on a stationary covariate, as required by the unit root test assumptions. By including the lagged vaccination roll-out, combined with the 7 day-average calculation adopted by OWID, we are able to account for the delayed effect of vaccines in containing the virus spread. Indeed, as shown in Bernal et al. [25], the impact on immunity was observed to occur after 14 days from the inoculation. In addition, by using a variable considering newly administered doses and not limiting to a specific one, e.g. first or second dose, we are able to assess the waning effect of vaccines on immunity. Hence, it is assumed that a constant amount of vaccinations is needed to control outbreaks, since it is unlikely to achieve a population coverage level according to which no more vaccinations are needed in case of occurrence of new virus variants in the short run. This is due to an unpredictable duration of vaccine effectiveness and virus mutations. Accordingly, the model is specifically useful at the beginning of a pandemic, where the highest part of a population is exposed to the new virus.

Concerning the Stringency Index, it is a composite measure developed by the Oxford COVID-19 Government Response Tracker (OxCGRT) to capture the degree of restrictiveness of non-pharmaceutical interventions (NPIs) implemented by governments during the COVID-19 pandemic. The index is constructed on a scale from 0 to 100, where higher values indicate more stringent policy responses, and it is derived from nine key indicators of government action, primarily focused on containment and closure policies: School and university closures, Workplace closures, Cancellation of public events, Restrictions on private gatherings, Public transport closures or restrictions, Stay-at-home requirements, Restrictions on internal movement, International travel controls, Public information campaigns. The Stringency index is designed to facilitate cross-country and temporal comparisons of policy stringency, rather than to directly assess policy effectiveness or epidemiological outcomes. As such, it has been used in empirical studies to explore associations between policy interventions, epidemiological trends, and socioeconomic impacts during the pandemic (see e.g. [26,27]).

Regarding the choice of sample countries, to get a broad overview of Europe in the pandemic context, we selected three countries per each European area according to the United Nations Statistics Division classification<sup>1</sup>:

- *Northern Europe*: Denmark, Sweden and United Kingdom;
- *Western Europe*: Austria, France and Germany;
- *Eastern Europe*: Bulgaria, Czechia and Poland;
- *Southern Europe*: Italy, Portugal and Spain.

Our data cover the period ranging from 1 February 2021 to 31 August 2022, to account for the impact of national vaccination roll-out and evolving virus variants, which started between the end of 2020 and the beginning of 2021 in most countries.

Across the four macro-areas, a diversified landscape of reactions was observed, with Western and Southern European countries that tended to deploy more centralized, rapid NPIs responses early in the pandemic, while some Northern and Eastern European

<sup>1</sup> <https://unstats.un.org/unsd/methodology/m49/>

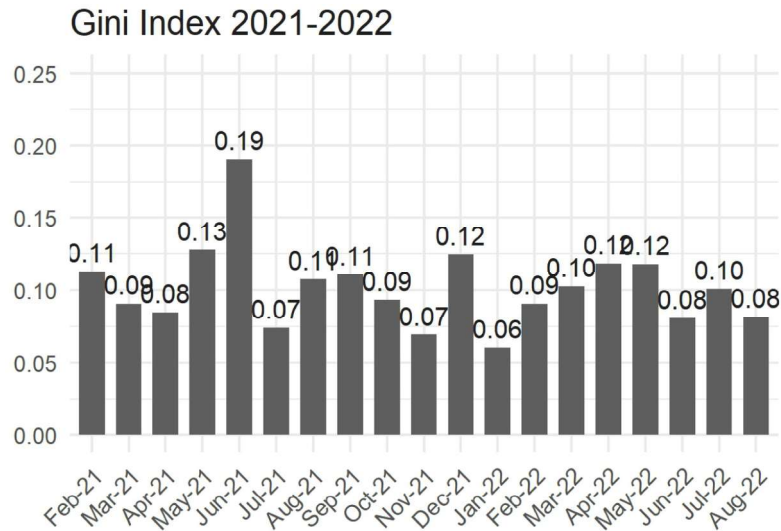


Fig. 1. Evolution of the Gini inequality index for the considered period and calculated at the country level. Gini ranges in  $[0;1]$  interval with 0 marking no inequality/concentration and 1 the highest possible inequality/concentration.

countries relied more on testing capacity, targeted restrictions, and regional adaptation in the first waves. The turning point across all contexts was the advent of vaccines, which reshaped risk assessments, enabled phased reopenings, and reduced severe disease and mortality even as transmission persisted.

More specifically, Northern Europe area saw Denmark and, to some extent, Sweden and the UK to relying on clear communication, public trust, and data-informed decisions to manage the balance between health measures and civil liberties. Precautionary testing, border measures, and adjustable NPIs helped in containing spread while trying to minimize prolonged restrictions.

Western Europe countries tended to opt for centralized or strongly coordinated approaches. They leaned on objective epidemiological or capacity-based thresholds to guide restrictions and relaxations. Robust testing infrastructures, digital contact tracing where feasible, and ambitious vaccination campaigns (including boosters) were central to maintaining health system resilience. From an economic point of view, large-scale fiscal measures and sector-specific aids were used to cushion restrictions, sustain livelihoods, and preserve public compliance.

Countries like Bulgaria and Czechia from Eastern Europe faced variability in hospital readiness and resources, which influenced the nature and timing of interventions. There was in place a recurring pattern of centralized guidance complemented by local adaptations to address regional epidemiology.

Finally, Southern Europe witnessed a rapid surge management with cross-regional coordination. While Italy highlighted cross-regional collaboration and hospital surge capacity, Spain and Portugal leveraged strong central-regional coordination to align interventions with epidemiological signals. The key element was that widespread vaccination campaigns, including boosters, were crucial to enabling safer reopenings.

To explore the possible effects of the diverse strategies adopted by countries in managing the pandemic, and in analogy with previous works like [28] and [29], who studied virus outbreaks through the lens of inequalities measures, we report in Fig. 1 the Gini inequality index assessed country-wise along the considered period, that is from February 2021 through August 2022. Each value refers to the amount of inequality among the countries in the average value of the reproduction rate with regards to a given considered month. We recall that the Gini index ranges between 0 and 1, where 0 means no concentration while 1 refers to maximum concentration. In our case, we find rather small values, from 0.06 to 0.19. It appears a quite evident pattern in the evolution, increasing phases followed by decreasing ones and a clear peak in June 2021 which indeed corresponds to the rise of a new wave in Europe. Moreover, the absence of a clear sign of concentration of the reproduction rate can be interpreted as underlying co-movements in the pandemic dynamics that tend to affect European countries in a similar way.

#### 4. Results

In this section, we show the results obtained by applying the testing approach presented in Section 2 to COVID-19 contagion data in 2021–2022 for the twelve considered countries.

The top panels of Figs. 2 through 7 show the  $p$ -value time series of the BSADF (blue line) and CBSADF explosivity tests (red line) applied to the effective reproduction number time series in the analyzed countries listed according to the alphabetical order. The  $p$ -values are obtained based on the critical values calculated through the bootstrap procedure by [16]. When the  $p$ -value is lower than the chosen significance levels (10% and 5% indicated, respectively, by the solid and dashed black lines), the test identifies the potential start of an explosive phase in the effective reproduction number, until the  $p$ -value returns above the significance level. By

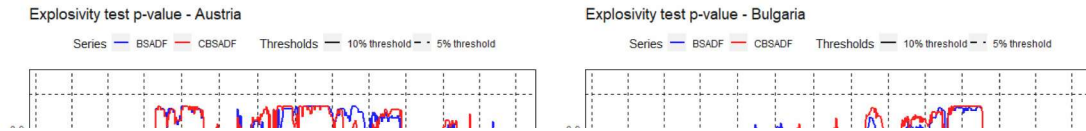


Fig. 2. Austria and Bulgaria. Top panels: p-values of the BSADF and CBSADF tests; the dashed and solid black lines represent the 5% and 10% significance thresholds, respectively. Bottom panels: reproduction rate (black line) and explosivity periods (shaded areas) as identified through the CBSADF testing procedure.

setting a minimum window length of 60 observations (according to the estimation approach described in Section 2), the first results can be calculated starting from April 2021. The bottom panels of Figs. 2 through 7 provide the identification of explosivity periods based on the calculated p-values, by showing, for each country, the reproduction rate time series and the identified explosivity periods, indicated as shaded areas. Indeed, for decision-making purposes, it is not enough to have a statistical signal (i.e.  $p$ -value below the chosen significance threshold) on a given day to declare the start of an explosive phase. Therefore, to avoid providing many false positive signals to the policymakers, the definition of explosive phase is more delimited than the one used in the standard CBSADF test procedure. Specifically, following Agosto and Cerchiello [14], we identify a warning signal if and only if two conditions are met for at least 5 days out of a 7-day window: 1) increased reproduction rate with respect to the previous day; 2) rejection of the null hypothesis of random walk, in favor of explosivity (active statistical signal). As a consequence, not all phases in which the statistical test signals the possible start of an explosive contagion phase are labeled as explosive (shaded areas in the bottom panels of Figs. 2 to 7). From the inspection of Figures from 2 to 7, it can be noticed that the CBSADF test signals explosive periods during late spring and summer 2021 – corresponding to the spread of the Delta variant – and the last months of 2021, when the Omicron variant caused a strong increase of infections. In particular, United Kingdom is the first country where the test detects the beginning of a wave, triggered by the spread of the Delta variant, in May 2021, followed by Portugal and Denmark, while for other countries, such as France, Italy and Bulgaria, the signal occurs later, in July. Among the considered countries, Czechia, Portugal and Poland show quite peculiar behavior, with several short-lasting explosivity signals. It can also be noticed that, in Sweden, an explosivity phase is signaled in the middle of May 2021, while the  $p$ -value drop, corresponding to the advent of the Delta wave in July, does not lead to a rejection of the random walk hypothesis in favor of the explosivity one.

Nevertheless, both tests provide an effective monitoring tool of the pandemic and, in most cases, the signal provided by the test with (CBSADF) and without (BSADF) covariate agrees, that is the two tests lead to the same inferential conclusion concerning the explosivity hypothesis. However, there are several points in time in which the two indicators diverge and the  $p$ -value of the CBSADF test is closer to the significance level, providing a potential warning indication about the contagion growth. Indeed, there are some cases in which the signal provided by the CBSADF test anticipates the one provided by the test without covariate.

A case where the signal provided by the two tests is different is that of Sweden at end of November/beginning of December 2021, when both tests show a rapid decrease of the  $p$ -value, but only the CBSADF test indicates the start of an explosivity phase lasting for some weeks, better capturing the rapid growth of the effective reproduction number in that period. In Germany, in September 2021, right before a new sharp increase in the effective reproduction number, the CBSADF test provides an explosivity signal, while

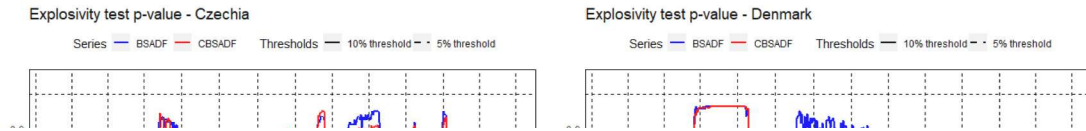


Fig. 3. Czechia and Denmark. Top panels: p-values of the BSADF and CBSADF tests; the dashed and solid black lines represent the 5% and 10% significance thresholds, respectively. Bottom panels: reproduction rate (black line) and explosivity periods (shaded areas) as identified through the CBSADF testing procedure.

the BSADF test does not. A partially different result for the two tests is obtained in Portugal at the beginning of November 2021, when the signal provided by the test with covariate is stronger and more persistent than the one provided by the baseline test. In Sweden, the test without covariate fails to recognize a short but steep rise in the effective reproduction number in December 2021. Interestingly, cases of temporary divergence between the two p-values, with the CBSADF test showing a lower  $p$ -value, closer to the explosivity threshold, are observed in the same period (fall 2021) in Germany, Italy, Denmark, and in Spain, where the divergence is stronger and starts when the summer descent of the effective reproduction number slows down, right before a new rise of infections. Finally, in Portugal, the test with covariate detects the rise of April 2021 in advance, with respect to the baseline version of the test.

It is worth remarking that, as a clear and exact definition of pandemic waves does not exist and, most of all, the waves tend to be labeled as such afterward by epidemiologists and local or national governments, a proper classification exercise which comprises the comparison between the actual classes (waves) and the predicted ones is not feasible. However, to show the correspondence between the signals provided by the CBSADF test and the phases of acceleration in contagion growth, as anticipated in the Introduction, we report in Table 1 the conclusions reached by the test in three phases corresponding to a strong growth of new infections in all countries: the one occurring with the spread of Delta variant (spring/summer 2021), the so-called Omicron wave (end of 2021/beginning of 2022) and the rise in reproduction rate observed in summer 2022. As it can be noticed, the signal is provided in all cases, except for Austria in the Omicron wave. Moreover, for Austria, France and Sweden in the Delta one and for Italy in the summer 2022 rise, the test provides a ‘quasi-signal’: the  $p$ -value shows a severe drop and goes close to the 10% threshold, without reaching it. In the case of Austria, the lack of signal in December 2021 is linked to the fact that the rising phase followed an equally rapid falling period. This particularly erratic dynamic leads the test not to consider the growth as explosive. For each detected signal, in Table 1 we also provide (in brackets) the number of days in which it remained active. It can be seen that the duration of the explosiveness warning signal is not homogeneous across countries and waves. On average, it lasted longest during the Delta wave – about 20 days – compared with roughly 17 days in Summer 2022 and 14 days in Omicron.

More generally, the test represents a real time approach to identify critical patterns in the evolution of the reproduction rate. Such patterns are signaled only if the increasing time series shows an explosive trait, according to the related econometric definition, and their identification should support, and not replace, a careful evaluation of the dynamics of infections.

Despite the considerations on the choice of vaccinations and in the light of robustness evaluation, rather than NPIs, as variables to be included in the explosivity test, we also perform the CBSADF test using the 7-day lagged first differences of the Stringency Index as a covariate and retrieved from the OWID data repository. The results – shown in the Appendix – indicate that, in this

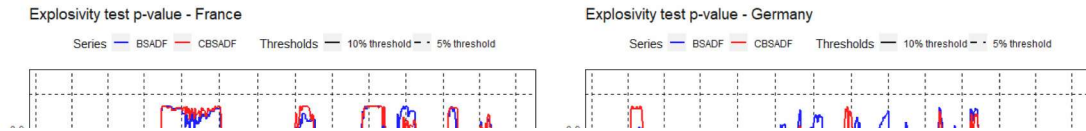


Fig. 4. France and Germany. Top panels: p-values of the BSADF and CBSADF tests; the dashed and solid black lines represent the 5% and 10% significance thresholds, respectively. Bottom panels: reproduction rate (black line) and explosivity periods (shaded areas) as identified through the CBSADF testing procedure.

case, the p-values of the BSADF and the CBSADF test are always almost perfectly overlapping, as it can be seen from Fig. A.1. In particular, Fig. A.1 reports the two tests'  $p$ -value for Italy, Portugal, Sweden and United Kingdom, countries characterized by different strategies in terms of both non-pharmaceutical countermeasures and vaccinations. Similar results were obtained for the remaining countries. This reveals that, in our sample, the Stringency Index does not show a significant relationship with the effective reproduction number and, thus, does not improve the monitoring of the pandemic. Such a result can also be induced by the fact that the Stringency Index measure suffers from inconsistencies and flaws, as it was meant to be a very quick and daily indicator at the expense of data quality standards.

A further proof of the importance of the role played by the vaccination roll-out, even in case of no difference in the signals between the BSADF and the CBSADF, is represented by the amount of extra variability of the effective reproduction number explained by that variable and measured through the  $R^2$  index. In particular, as a supplementary analysis, we extract the  $R^2$  indexes from the dynamic linear regression models underlying the tests. For the sake of clarity, we recall that in the basic model – corresponding to the BSADF assumptions – the only regressor is the lagged dependent variable, while in the counterpart that mimics the CBSADF dynamics the additional regressor is the change in daily new vaccinations. Figures from A.2 through A.7 show the difference in the  $R^2$  indexes between the two above-mentioned models. According to the considered country and period, we can observe differences in the  $R^2$  indexes with peaks above 30% (see for example Austria, Denmark, Germany, Spain and UK), and more in general several significant differences, in favor of the covariate-augmented model. Such results support again the opportunity of considering the covariate augmented test and are confirmed by the values of Akaike (AIC) and Bayesian (BIC) information criteria computed in correspondence to the peaks in the adjusted  $R^2$  change – reported in Table A.1 – showing the superiority of the CBSADF model. One last aspect that is worth considering pertains to the possible role played by the vaccination roll-out in effectively containing and restraining the evolution of pandemic waves. As the reader can spot from Figs. A.8 through A.13, there are several phases in which the vaccination coefficient is negative and significant. This implies that vaccination is contributing to reducing the effective reproduction number. That said, it is even more interesting to evaluate possible phases in which the tests signal explosivity and the vaccination has a significant and negative impact. In such phases we can infer that without vaccination the waves would have been even more severe. To summarize the presence and timing of such phases in the different countries, in Table A.2 we report, for each country, the months in which tests and negative signs match and how many times this occurs. It appears as a common trait among the countries that vaccination was pivotal during the summer 2021 (Delta wave) and the end of the year 2021 (Omicron wave).

The analysis of correlation between the reproduction rate and the vaccination roll-out confirm the previous findings. In fact, the values of Pearson correlations – together with the associated t-statistics – over the time windows analyzed in our study (Figs.



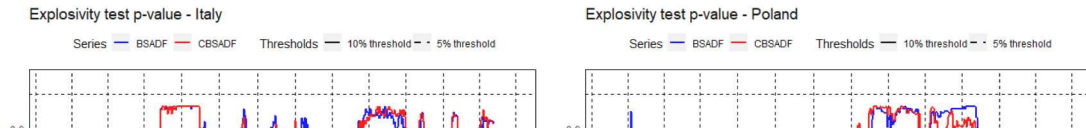


Fig. 5. Italy and Poland. Top panels: p-values of the BSADF and CBSADF tests; the dashed and solid black lines represent the 5% and 10% significance thresholds, respectively. Bottom panels: reproduction rate (black line) and explosivity periods (shaded areas) as identified through the CBSADF testing procedure.

A.14 through A.25), show that, as expected, while spurious positive correlations prevail in non-explosive growth times, negative and significant coefficients characterize the phases of exponential growth representing possible new waves (see Figs. 3–6).

## 5. Robustness analysis

For comparative and robustness purposes, we considered a possible alternative for the identification of explosive patterns. The well-known paper by [30] proposed an approach to the identification of complexity of temporal properties in longitudinal data. In particular, the authors suggested a measure called burstiness, based on the estimation of a parameter ( $B$ ) that quantifies the degree of irregularity in the timing of events and can be used to identify periods of rapid, clustered events followed by long gaps of inactivity. Assuming the existence of a system whose components have a measurable activity pattern that can be transformed into a discrete signal, by recording the moments when some events take place, the burstiness parameter  $B$  is measured using the mean ( $\mu$ ) and standard deviation ( $\sigma$ ) of the inter-event time distribution, as shown below:

$$B = \frac{\sigma - \mu}{\sigma + \mu} \quad (9)$$

In this sense, the calculation of the  $B$  parameter on a daily basis enables the monitoring of the activity patterns of the reproduction rate and allows a direct comparison with our approach. Specifically, analogously to our testing procedure, the  $B$  parameter can be calculated for each day through a rolling-windows approach, providing a detailed control on the evolution patterns of the  $R_t$  time series. The parameter  $B$  ranges between  $-1$  and  $1$ : values closer to  $-1$  indicate more regular intervals between events, values near  $0$  suggest a random distribution, and values closer to  $1$  reflect a more pronounced burst pattern. Since the  $B$  measure must be computed from a discrete series of events, we map the continuous reproduction rate variable into a dichotomous one using a thresholding mechanism. To this end, we evaluated several candidate thresholds for defining an “event”, understood as a significant increase in the reproduction rate. The values considered were  $[0.01, 0.05, 0.15, 0.02]$ , and a comparative assessment across all countries identified  $0.01$  as the optimal threshold.

Figs. 8, 9, and 10 show, for each country analyzed, the time series of the  $B$  parameter, estimated using 60-day rolling windows (corresponding to the minimum window length required for our test, as described in Section 2). Across all countries, burstiness values range between  $-1$  and  $0.48$ , reflecting an alternation of regular, random, and markedly bursty periods, depending on the underlying dynamics of the reproduction rate. The most explosive phases of the pandemic – namely the summer 2021 and late 2021/early 2022

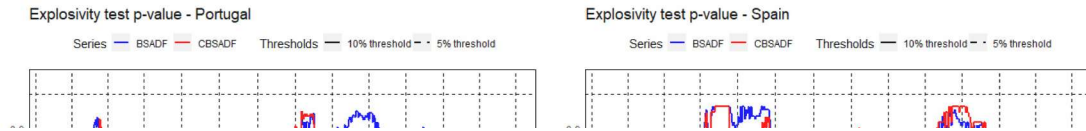


Fig. 6. Portugal and Spain. Top panels: p-values of the BSADF and CBSADF tests; the dashed and solid black lines represent the 5% and 10% significance thresholds, respectively. Bottom panels: reproduction rate (black line) and explosivity periods (shaded areas) as identified through the CBSADF testing procedure.

waves – are partially captured by the [30] method, as reflected in a general increase of the burstiness parameter toward 0.5 (still far from the maximum value of 1). However, such signals can properly emerge only in retrospective assessments. More specifically, the burstiness analysis depends upon the definition of an “event”, that is not trivial when dealing with continuous variables. More specifically, burstiness analysis depends critically on how an “event” is defined, which is straightforward for discrete data (e.g., the sending of an email or the translation of a protein, as in the original paper by Goh and Barabási [30]), but much less so when applied to continuous variables. In the context of pandemic data, relevant variables are continuous, requiring an ad hoc mapping that is difficult to implement in an online monitoring scheme. A comparative evaluation of thresholds can be conducted retrospectively, once sufficiently long time series are available. A seemingly natural threshold is  $R_t > 1$ , which typically marks explosive dynamics in the pandemic’s evolution. However, this criterion would identify far fewer events and, more importantly, would signal the onset of critical phases with substantial delay. Moreover, in order to employ burstiness analysis for pandemic monitoring, policymakers would need to establish not only the threshold defining an “event”, but also the threshold for the B parameter above which the level of burstiness should be regarded as critical or severe.

Finally, our test-based approach is inferential by design, as it automatically provides standard errors and p-values for the estimated autoregressive coefficient on which the test relies. By contrast, burstiness analysis can only be made inferential through a bootstrapping strategy.

## 6. Discussion

This paper investigates the idea of combining epidemic surge detection with the study of the role of vaccination roll-out. Explosivity tests have already been proven to be a useful tool to provide early signals at the beginning of pandemic waves [14]. In the context of SIR models [5] and agent based modeling [6,7], this approach enables a status quo evaluation of the pandemic evolution without particular assumptions, while SIR models and agent-based modeling are useful to estimate the future development by showing how different measures might affect the possible patterns [6,7]. Further, it is expected that the precision of BSADF tests can be further improved by adding covariates, as the present study has demonstrated.

Our results indicate that the proposed testing approach represents a reliable – and statistically robust – tool to monitor the pandemic phases and that considering the progress of national vaccination roll-out as a covariate, provides a more powerful signal for new waves’ identification. In comparison to the BSADF test, the CBSADF test has been proven to be more sensitive. On the one

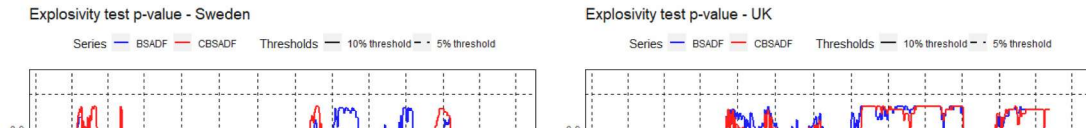


Fig. 7. Sweden and United Kingdom. Top panels: p-values of the BSADF and CBSADF tests; the dashed and solid black lines represent the 5% and 10% significance thresholds, respectively. Bottom panels: reproduction rate (black line) and explosivity periods (shaded areas) as identified through the CBSADF testing procedure.

hand, it provides signals earlier in some cases and, on the other hand, it even reveals significant increases where the BSADF test does not. Furthermore, by considering the changes in  $R^2$ , it can be seen that the variability is better explained by the CBSADF model.

However, whether the CBSADF approach is superior to BSADF depends on the availability and choice of appropriate covariates. Indeed, if a covariate has a weak and/or unstable relationship with the target variable on which explosivity is tested, the two tests provide a very similar signal. The Stringency Index, for example, turned out not to be a useful covariate to be included in our testing procedure, since it provides no improvement in wave detection compared to the BSADF model. Furthermore, the Stringency Index comprises a mix of non-pharmaceutical measures, making it difficult to draw conclusions on the direct impact of each specific countermeasure. By contrast, vaccination rollout can be easily interpreted and, as shown in this study, can represent an alert warning signal for explosive behaviors.

Overall, the CBSADF model has proven to be a useful method to predict pandemic waves at the beginning of their occurrence in order to allow the timely introduction of measures at an early stage. In cases where reliable data capable of detecting pandemic development are available, the CBSADF approach delivers more accurate signals and, additionally, provides insight into the role of the employed covariate. If a proper covariate is not available – for example, if vaccination has not been developed yet or data quality is poor – the BSADF approach can be used, since it still provides reliable results. Moreover, even if there is no approved approach in the literature to mark the beginning of a pandemic wave when it starts to happen, for comparative purposes we have also considered an alternative strategy based on the well-known paper by Goh and Barabási [30]. By means of the burstiness parameter  $B$  calculated according to a rolling-windows strategy, we were able to directly assess the relative results. We found that the alternative strategy can identify some explosive patterns, but this heavily depends on both the minimal ideal value of  $B$  to signal the beginning of a critical phase and on the strategy used to define the events. Policymakers could face issues in deploying a proper online monitoring system of a pandemic that depends on such decisions.

In addition, we acknowledge the limitations of our work: both tests might be too sensitive to noisy patterns in the data, even if there is no strong, prolonged increase in the reproduction rate. Nevertheless, this also depends upon the quality of the data and specifically on the covariate used to model the evolution of the reproduction rate. Being aware of such limitation, it is recommended to employ the test in combination with supplementary epidemiological indicators so to provide policymakers with a kind of control dashboard equipped with an up-to-date and robust set of information. Using newly administered vaccines as covariate might only be appropriate in the specific case of SARS-Cov-2, since waning immunity and the necessity of booster doses have been shown in

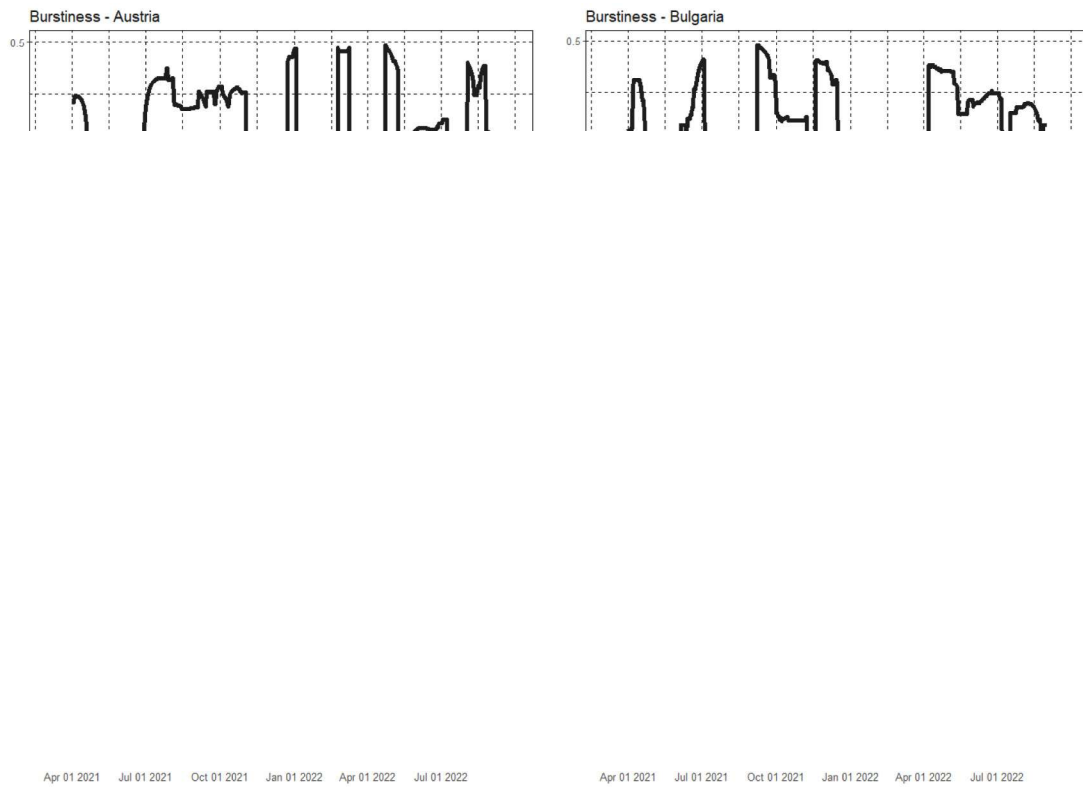


**Fig. 8.** Austria, Bulgaria, Czechia and Denmark. Time series of estimated burstiness parameters  $B$ .

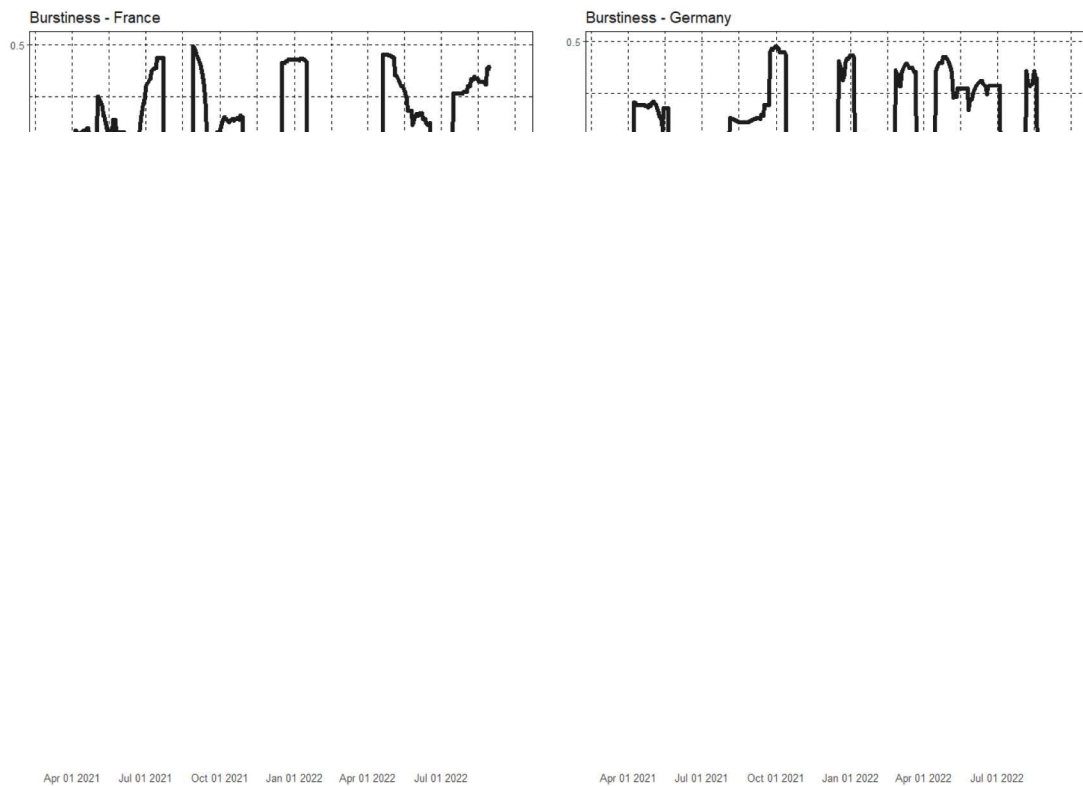


**Fig. 9.** France, Germany, Italy and Poland. Time series of estimated burstiness parameters  $B$ .

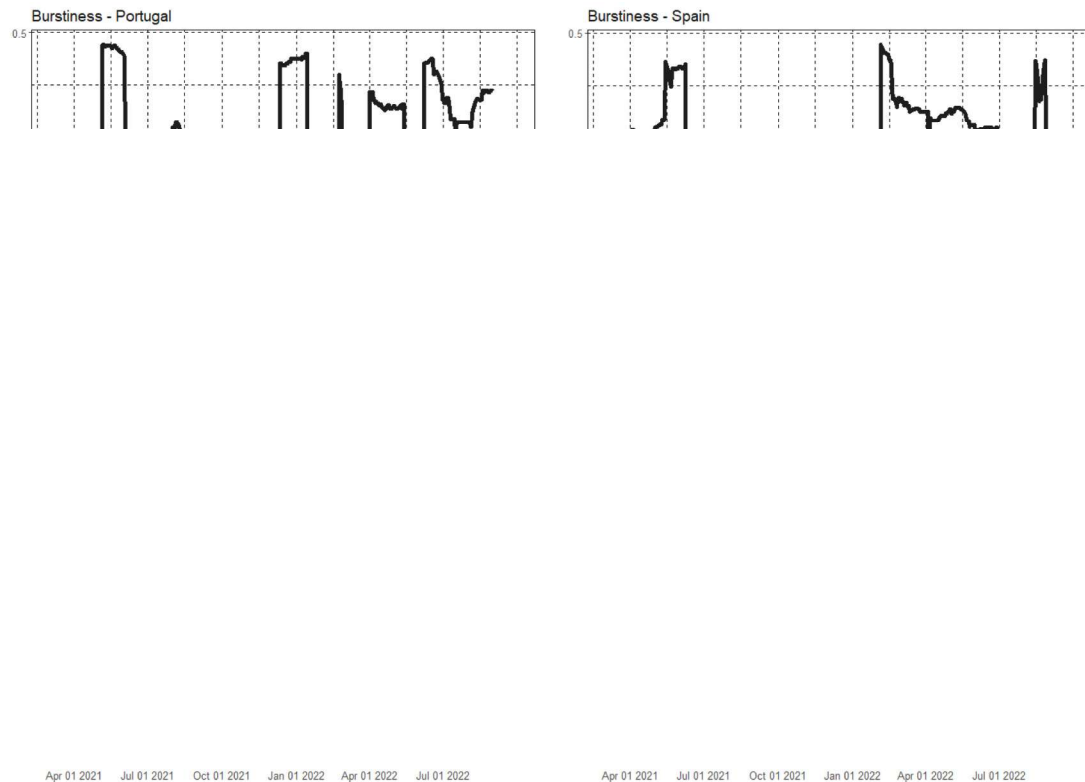


Fig. 10. Portugal, Spain, Sweden and United Kingdom. Time series of estimated burstiness parameters B.

many studies (e.g. Krueger et al. 2022), but might be different for other vaccinations or upcoming diseases. Consequently, covariates have to be chosen based on available information for specific diseases.

Further development of the present study would consider the inclusion of a larger set of countries, ideally outside the European continent, to further assess the robustness of the approach. Nevertheless, in case other relevant variables were made available, the CBSADF test could be profitably employed.

#### CRedit authorship contribution statement

**Arianna Agosto:** Writing – review & editing, Writing – original draft, Methodology, Conceptualization. **Paola Cerchiello:** Writing – review & editing, Writing – original draft, Methodology, Conceptualization. **Siegfried Eisenberg:** Writing – review & editing, Writing – original draft, Conceptualization. **Thomas Czypionka:** Writing – review & editing, Writing – original draft, Conceptualization.

#### Declaration of competing interest

The authors declare that they have no known competing financial interests or personal relationships that could have appeared to influence the work reported in this paper.

#### Acknowledgments

The authors received funding from the European Union's Horizon 2020 research and innovation programme under grant agreement No. 101016233 (PERISCOPE).

#### Appendix A

See [Figs. A.3–A.6](#), [A.9–A.12](#), [A.14](#) and [A.16–A.24](#).



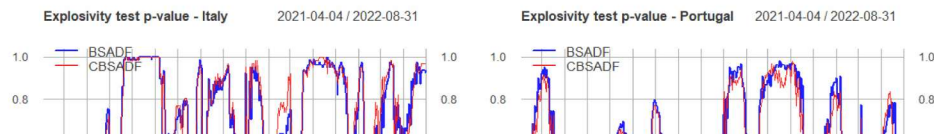


**Fig. A.1.** Test results when the Stringency Index variable is included as covariate in the CBSADF test. From top left to bottom right: Italy, Portugal, Sweden and United Kingdom.

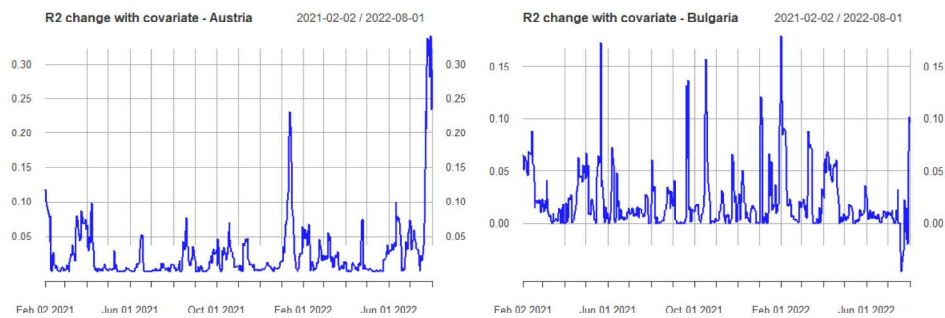


**Fig. A.2.** Austria (left) and Bulgaria (right): change in model R-squared when the vaccination covariate is included.

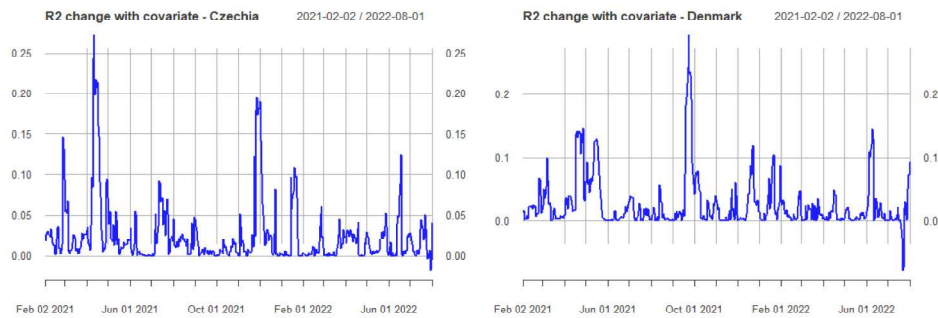


**Fig. A.3.** Czechia (left) and Denmark (right): change in model R-squared when the vaccination covariate is included.

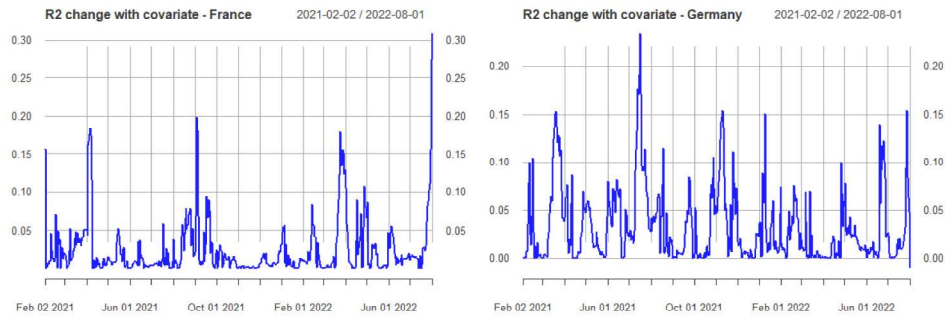


Fig. A.4. France (left) and Germany (right): change in model R-squared when the vaccination covariate is included.

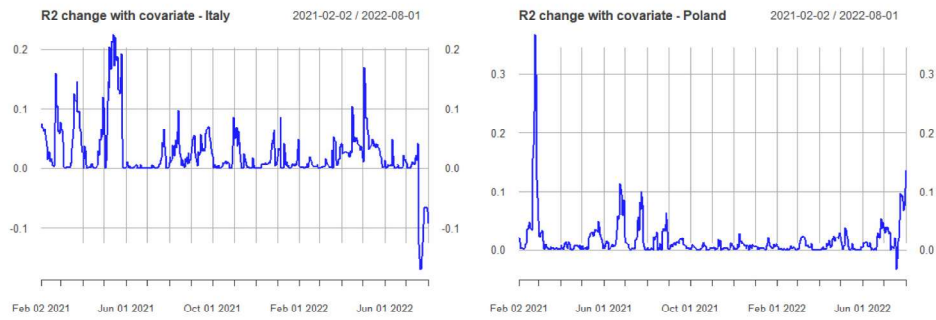


Fig. A.5. Italy (left) and Poland (right): change in model R-squared when the vaccination covariate is included.

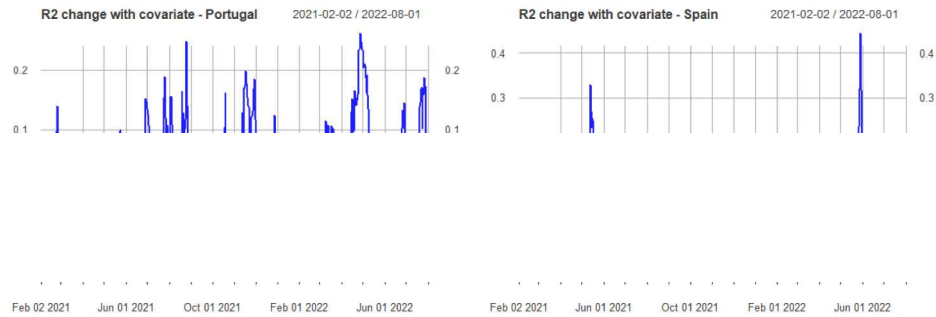


Fig. A.6. Portugal (left) and Spain (right): change in model R-squared when the vaccination covariate is included.

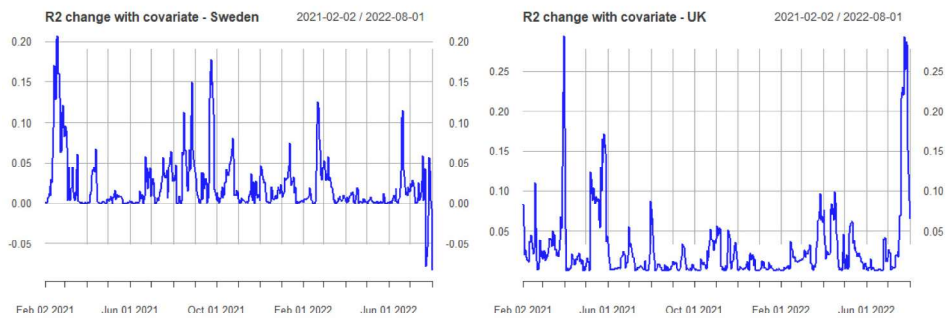
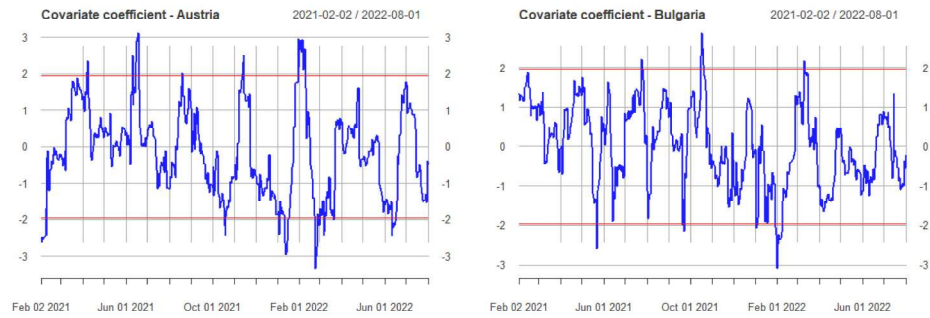
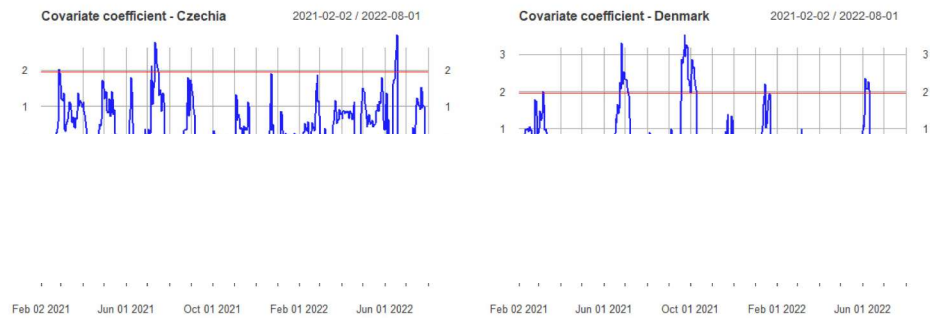


Fig. A.7. Sweden (left) and United Kingdom (right): change in model R-squared when the vaccination covariate is included.



**Fig. A.8.** Austria (left) and Bulgaria (right): t-statistic of the coefficient associated to the vaccination roll-out covariate. The red lines mark the 5% significance level.



**Fig. A.9.** Czechia (left) and Denmark (right): t-statistic of the coefficient associated to the vaccination roll-out covariate. The red lines mark the 5% significance level.

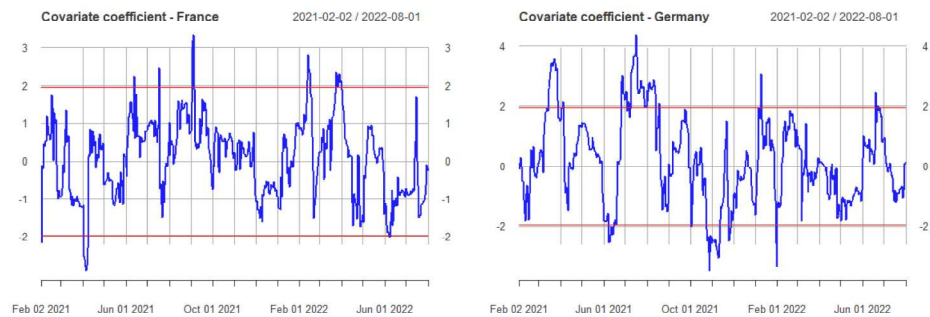


**Fig. A.10.** France (left) and Germany (right): t-statistic of the coefficient associated to the vaccination roll-out covariate. The red lines mark the 5% significance level.

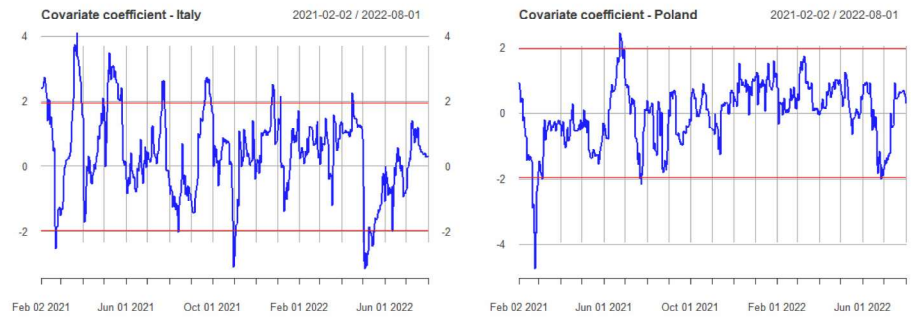


**Fig. A.11.** Italy (left) and Poland (right): t-statistic of the coefficient associated to the vaccination roll-out covariate. The red lines mark the 5% significance level.

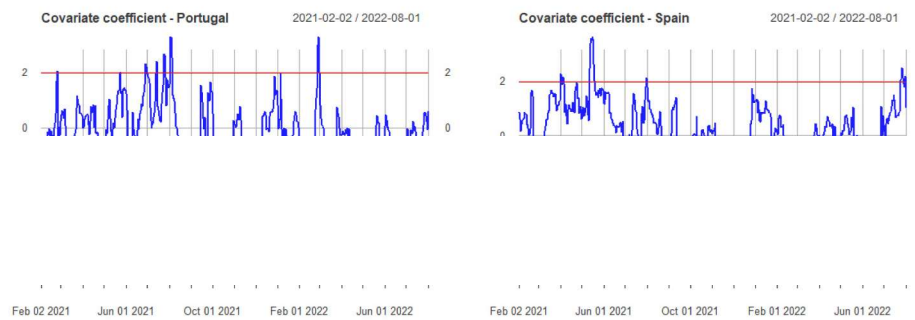


**Fig. A.12.** Portugal (left) and Spain (right): t-statistic of the coefficient associated to the vaccination roll-out covariate. The red lines mark the 5% significance level.

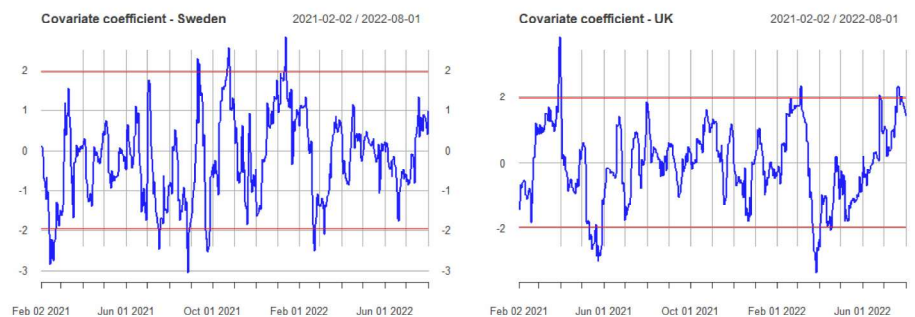


**Fig. A.13.** Sweden (left) and United Kingdom (right): t-statistic of the coefficient associated to the vaccination roll-out covariate. The red lines mark the 5% significance level.

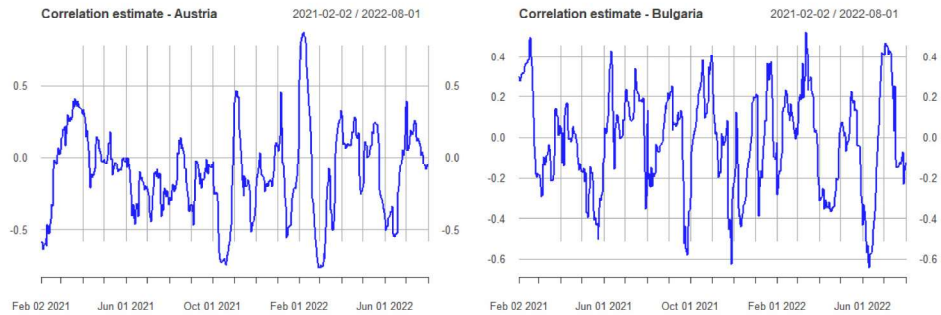


Fig. A.14. Austria (left) and Bulgaria (right): values of correlation between the reproduction rate and the new vaccinations variable.

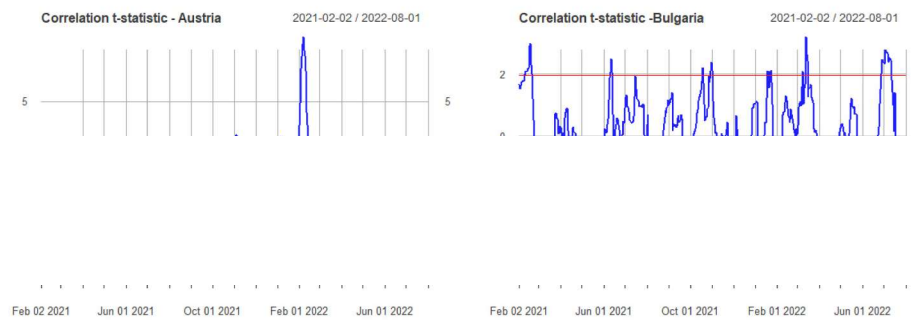


Fig. A.15. Austria (left) and Bulgaria (right): t-statistics of correlation between the reproduction rate and the new vaccinations variable. The red lines mark the 5% significance level.

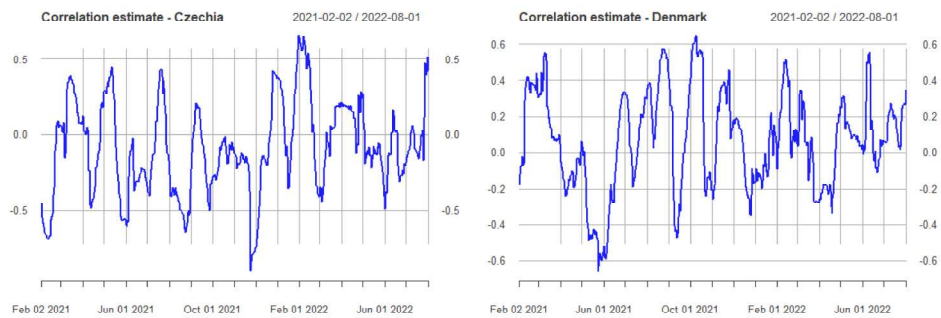
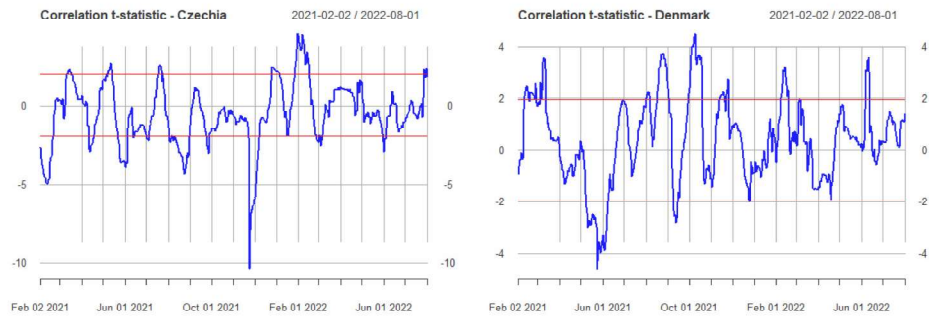
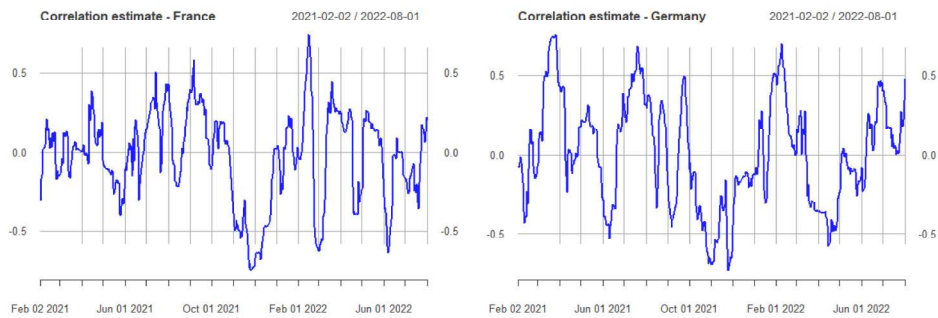


Fig. A.16. Czechia (left) and Denmark (right): values of correlation between the reproduction rate and the new vaccinations variable.





**Fig. A.17.** Czechia (left) and Denmark (right): t-statistics of correlation between the reproduction rate and the new vaccinations variable. The red lines mark the 5% significance level.



**Fig. A.18.** France (left) and Germany (right): values of correlation between the reproduction rate and the new vaccinations variable.

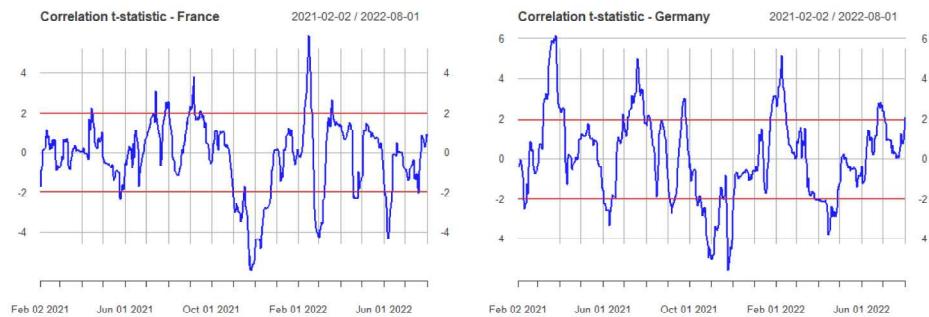


**Fig. A.19.** France (left) and Germany (right): t-statistics of correlation between the reproduction rate and the new vaccinations variable. The red lines mark the 5% significance level.

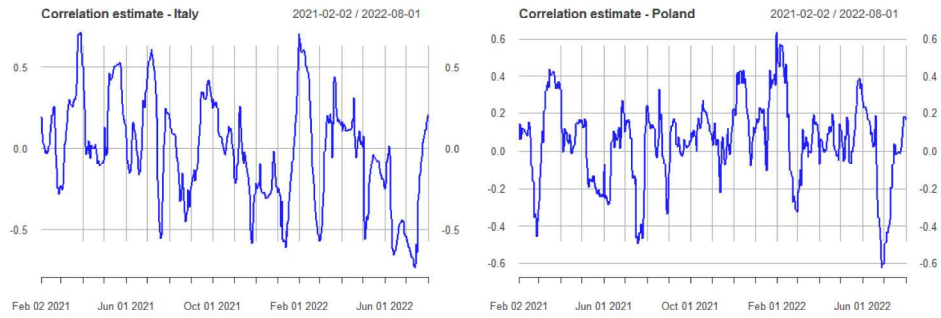


**Fig. A.20.** Italy (left) and Poland (right): values of correlation between the reproduction rate and the new vaccinations variable.

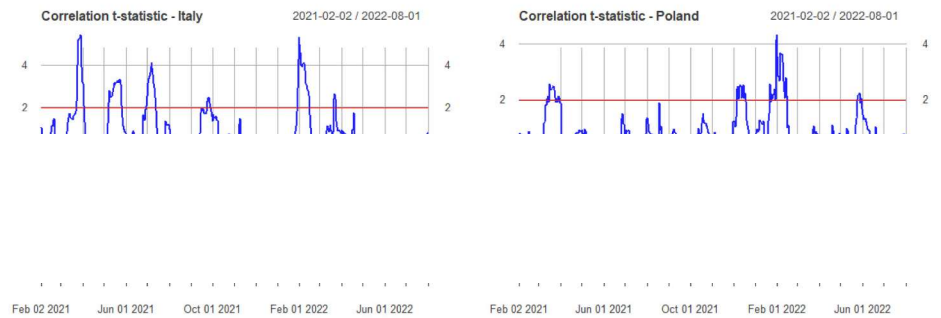


**Fig. A.21.** Italy (left) and Poland (right): t-statistics of correlation between the reproduction rate and the new vaccinations variable. The red lines mark the 5% significance level.

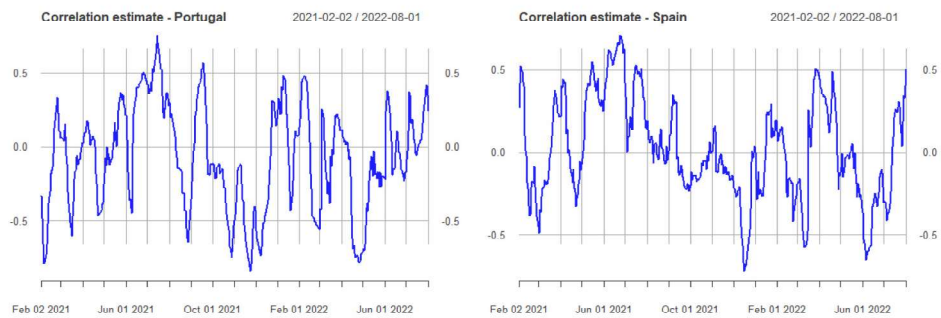


**Fig. A.22.** Portugal (left) and Spain (right): values of correlation between the reproduction rate and the new vaccinations variable.

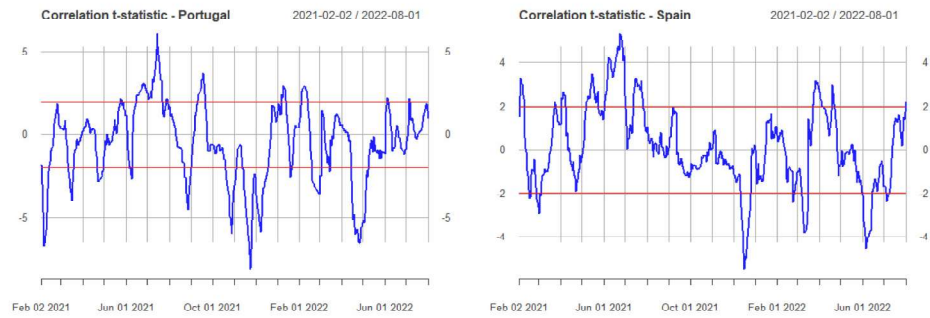


**Fig. A.23.** Portugal (left) and Spain (right): t-statistics of correlation between the reproduction rate and the new vaccinations variable. The red lines mark the 5% significance level.

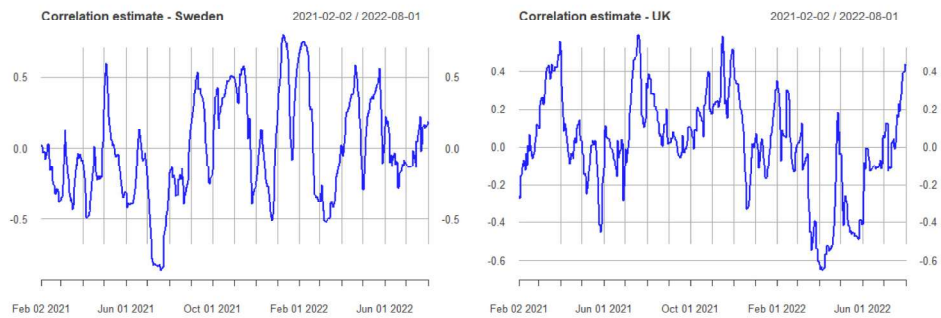


**Fig. A.24.** Sweden (left) and United Kingdom (right): values of correlation between the reproduction rate and the new vaccinations variable.

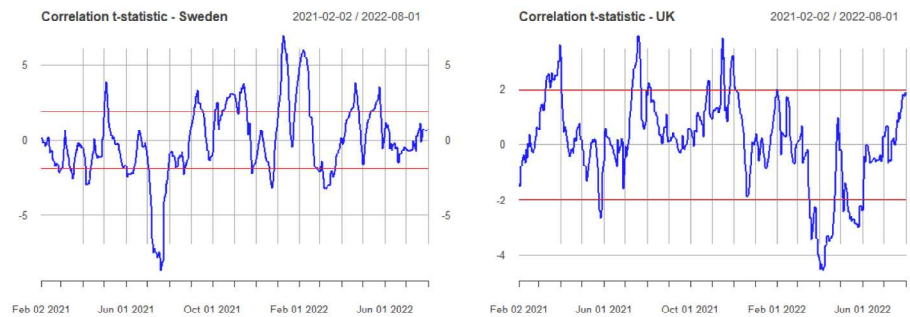


**Fig. A.25.** Sweden (left) and United Kingdom (right): t-statistics of correlation between the reproduction rate and the new vaccinations variable. The red lines mark the 5% significance level.

**Table A.1**

Akaike (AIC) and Bayesian (BIC) information criteria corresponding to the maximum peak in adjusted R-squared change reached by including the vaccination covariate.

Country	AIC		BIC	
	Without cov.	With cov.	Without cov.	With cov.
Austria	−190.30	−197.29	−183.64	−189.29
Bulgaria	−194.05	−198.11	−188.44	−192.28
Czechia	−204.08	−212.13	−197.42	−204.14
Denmark	−212.22	−212.53	−204.23	−205.87
France	−196.51	−204.66	−189.85	−196.66
Germany	−177.96	−192.79	−171.29	−184.79
Italy	−185.49	−193.32	−178.83	−185.32
Poland	−165.85	−177.57	−158.22	−164.77
Portugal	−174.89	−187.75	−168.23	−179.76
Spain	−162.78	−181.75	−156.12	−173.76
Sweden	−195.93	−201.98	−189.27	−193.99
United Kingdom	−215.35	−226.99	−208.69	−219.00

**Table A.2**

For each country, the months in which tests and negative signs match and how many times this occurs.

Country	Phases of negative significant coefficient	# Phases of negative significant coefficient
Austria	Jun. '22	1
Bulgaria	May '21 – Sep. '21 – Jan/Feb. '22	3
Czechia	Apr. '21 – Nov/Dec. '21 – Jan. '22	3
Denmark	–	0
France	Jun. '22	1
Germany	Jun. '21 – Dec. '21 – Feb. '22	3
Italy	Aug. '21 – Nov. '21	2
Poland	Jan/Feb. '21 – Jul. '21	2
Portugal	Aug. '21 – Oct. '21 – Dic. '21 – May '22 – Jul. '22	5
Spain	Dec. '21 – Jun. '22	2
Sweden	Jul. '21 – Oct. '21 – Apr. '22	3
UK	May/Jun. '21	1

## Data availability

Data are publicly available at the link specified in the manuscript (<https://github.com/owid/covid-19-data/tree/master/public/data>).

## References

- [1] K. Koelle, M.A. Martin, R. Antia, B. Lopman, N.E. Dean, The changing epidemiology of SARS-CoV-2, *Science* 375 (6585) (2022) 1116–1121.
- [2] C. Amuedo-Dorantes, N. Kaushal, A.N. Muchow, Timing of social distancing policies and COVID-19 mortality: county-level evidence from the US, *J. Popul. Econ.* 34 (2021) 1445–1472.
- [3] J.D. Sachs, S.S.A. Karim, L. Akin, J. Allen, K. Brosbøl, F. Colombo, G.C. Barron, M.F. Espinosa, V. Gaspar, A. Gaviria, et al., The lancet Commission on lessons for the future from the COVID-19 pandemic, *Lancet* 400 (10359) (2022) 1224–1280.
- [4] G. Chowell, L. Sattenspiel, S. Bansal, C. Viboud, Mathematical models to characterize early epidemic growth: A review, *Phys. Life Rev.* 18 (2016) 66–97.
- [5] C. Ji, D. Jiang, Threshold behaviour of a stochastic SIR model, *Appl. Math. Model.* 38 (21–22) (2014) 5067–5079.
- [6] B.D. Marshall, S. Galea, Formalizing the role of agent-based modeling in causal inference and epidemiology, *Am. J. Epidemiol.* 181 (2) (2015) 92–99.
- [7] M. Tracy, M. Cerdá, K.M. Keyes, Agent-based modeling in public health: current applications and future directions, *Annu. Rev. Public. Health* 39 (2018) 77–94.
- [8] C.C. Kerr, R.M. Stuart, D. Mistry, R.G. Abeysuriya, K. Rosenfeld, G.R. Hart, R.C. Núñez, J.A. Cohen, P. Selvaraj, B. Hagedorn, et al., Covasim: an agent-based model of COVID-19 dynamics and interventions, *PLoS Comput. Biol.* 17 (7) (2021) e1009149.
- [9] J. Lasser, T. Hell, D. Garcia, Assessment of the effectiveness of Omicron transmission mitigation strategies for European universities using an agent-based network model, *Clin. Infect. Dis.* 75 (12) (2022) 2097–2103.
- [10] N.E. Kogan, L. Clemente, P. Liautaud, J. Kaashoek, N.B. Link, A.T. Nguyen, F.S. Lu, P. Huybers, B. Resch, C. Havas, et al., An early warning approach to monitor COVID-19 activity with multiple digital traces in near real time, *Sci. Adv.* 7 (10) (2021) eabd6989.
- [11] L. Alessandretti, What human mobility data tell us about COVID-19 spread, *Nat. Rev. Phys.* 4 (1) (2022) 12–13.
- [12] F. Amman, R. Markt, L. Endler, S. Hupfaut, B. Agerer, A. Schedl, L. Richter, M. Zechmeister, M. Bicher, G. Heiler, et al., Viral variant-resolved wastewater surveillance of SARS-CoV-2 at national scale, *Nature Biotechnol.* 40 (12) (2022) 1814–1822.
- [13] J. Harvey, B. Chan, T. Srivastava, A.E. Zarebski, P. Dlotko, P. Błaszczuk, R.H. Parkinson, L.J. White, R. Aguas, A. Mahdi, Epidemiological waves-types, drivers and modulators in the COVID-19 pandemic, *Heliyon* 9 (5) (2023).
- [14] A. Agosto, P. Cerchiello, A data-driven test approach to identify COVID-19 surge phases: an alert-warning tool, *Statistics* (2024) 1–15.
- [15] P.C. Phillips, J. Yu, Dating the timeline of financial bubbles during the subprime crisis, *Quant. Econ.* 2 (3) (2011) 455–491.
- [16] S. Astill, A.R. Taylor, N. Kellard, I. Korkos, Using covariates to improve the efficacy of univariate bubble detection methods, *J. Empir. Financ.* 70 (2023) 342–366.
- [17] B.E. Hansen, Rethinking the univariate approach to unit root testing: Using covariates to increase power, *Econometric Theory* 11 (5) (1995) 1148–1171.

- [18] D.A. Dickey, W.A. Fuller, Distribution of the estimators for autoregressive time series with a unit root, *J. Amer. Statist. Assoc.* 74 (366a) (1979) 427–431.
- [19] J. Fry, E.-T. Cheah, Negative bubbles and shocks in cryptocurrency markets, *Int. Rev. Financ. Anal.* 47 (2016) 343–352.
- [20] S. Corbet, B. Lucey, A. Urquhart, L. Yarovaya, Cryptocurrencies as a financial asset: A systematic analysis, *Int. Rev. Financ. Anal.* 62 (2019) 182–199.
- [21] A. Agosto, P. Cerchiello, P. Pagnottoni, Sentiment, Google queries and explosivity in the cryptocurrency market, *Phys. A* 605 (2022) 128016.
- [22] P.C. Phillips, S. Shi, J. Yu, Testing for multiple bubbles: Historical episodes of exuberance and collapse in the S&P 500, *Internat. Econom. Rev.* 56 (4) (2015) 1043–1078.
- [23] G.M. Caporale, N. Pittis, Unit root testing using covariates: some theory and evidence, *Oxf. Bull. Econ. Stat.* 61 (4) (1999) 583–595.
- [24] F. Arroyo-Marioli, F. Bullano, S. Kucinskas, C. Rondón-Moreno, Tracking R of COVID-19: A new real-time estimation using the Kalman filter, *PloS One* 16 (1) (2021) e0244474.
- [25] J.L. Bernal, N. Andrews, C. Gower, C. Robertson, J. Stowe, E. Tessier, R. Simmons, S. Cottrell, R. Roberts, M. O'Doherty, et al., Effectiveness of the Pfizer-BioNTech and Oxford-AstraZeneca vaccines on covid-19 related symptoms, hospital admissions, and mortality in older adults in England: test negative case-control study, *Br. Med. J.* 373 (2021).
- [26] N. Islam, S.J. Sharp, G. Chowell, S. Shabnam, I. Kawachi, B. Lacey, J.M. Massaro, R.B. D'Agostino, M. White, Physical distancing interventions and incidence of coronavirus disease 2019: natural experiment in 149 countries, *Br. Med. J.* 370 (2020).
- [27] T. Hale, N. Angrist, R. Goldszmidt, B. Kira, A. Petherick, T. Phillips, S. Webster, E. Cameron-Blake, L. Hallas, S. Majumdar, et al., A global panel database of pandemic policies (Oxford COVID-19 Government Response Tracker), *Nat. Hum. Behav.* 5 (4) (2021) 529–538.
- [28] J. Abeles, D.J. Conway, The gini coefficient as a useful measure of malaria inequality among populations, *Malar. J.* 19 (1) (2020) 444.
- [29] U. Samarasekera, Inequalities hinder infectious disease control, *Lancet Infect. Dis.* 22 (2) (2022) 172.
- [30] K.-I. Goh, A.-L. Barabási, Burstiness and memory in complex systems, *Europhys. Lett.* 81 (4) (2008) 48002.